

UC Berkeley

UC Berkeley Previously Published Works

Title

Enhanced tropical methane production in response to iceberg discharge in the North Atlantic

Permalink

<https://escholarship.org/uc/item/8sm2s5cp>

Journal

Science, 348(6238)

ISSN

0036-8075

Authors

Rhodes, Rachael H
Brook, Edward J
Chiang, John CH
[et al.](#)

Publication Date

2015-05-29

DOI

10.1126/science.1262005

Peer reviewed

Enhanced tropical methane production in response to iceberg discharge in the North Atlantic

1. **Rachael H. Rhodes^{1,*},**
2. **Edward J. Brook¹,**
3. **John C. H. Chiang²,**
4. **Thomas Blunier³,**
5. **Olivia J. Maselli⁴,**
6. **Joseph R. McConnell⁴,**
7. **Daniele Romanini⁵,**
8. **Jeffrey P. Severinghaus⁶**

See all authors and affiliations

DOI: 10.1126/science.1262005

- [Article](#)
- [Figures & Data](#)
- [Info & Metrics](#)
- [eLetters](#)
- [PDF](#)

The tropical impact of iceberg armadas

The massive discharges of icebergs from the Greenland ice sheet during the Last Glacial Period are called Heinrich events. But did Heinrich events cause abrupt climate change, or were they a product of it? Methane levels represent a proxy for climate, because methane production increases mostly due to wetter conditions in the tropics. Rhodes *et al.* report a highly resolved record of atmospheric methane concentrations, derived from an ice core from Antarctica. Methane levels varied—i.e., the tropical climate changed—in response to cooling in the Northern Hemisphere caused by Heinrich events.

Science, this issue p. [1016](#)

Abstract

The causal mechanisms responsible for the abrupt climate changes of the Last Glacial Period remain unclear. One major difficulty is dating ice-rafted debris deposits associated with Heinrich events: Extensive iceberg influxes into the North Atlantic Ocean linked to global impacts on climate and biogeochemistry. In a new ice core record of atmospheric methane with ultrahigh temporal resolution, we find abrupt methane increases within Heinrich stadials 1, 2, 4, and 5 that, uniquely, have no counterparts in

Greenland temperature proxies. Using a heuristic model of tropical rainfall distribution, we propose that Hudson Strait Heinrich events caused rainfall intensification over Southern Hemisphere land areas, thereby producing excess methane in tropical wetlands. Our findings suggest that the climatic impacts of Heinrich events persisted for 740 to 1520 years.

Paleoclimate proxy evidence suggests that the climatic impacts of Heinrich events extended far beyond the North Atlantic basin ([1](#)). Enduring questions include whether Heinrich events initiated climate change or occurred in response to it, and how they may be linked to abrupt millennial-scale climate oscillations, typified by Dansgaard-Oeschger (DO) cycles in Greenland ice cores ([2](#)). Early correlation between DO cycle variability and sea surface temperature (SST) proxies found that Heinrich events occurred within the coldest, longest stadials of the Greenland $\delta^{18}\text{O}_{\text{ice}}$ record ([3](#)), referred to as Heinrich stadials (HSs) 1 to 6. This correlation could suggest causation: The addition of fresh water causes a shutdown of the Atlantic meridional overturning circulation (AMOC) and prolonged cold conditions ([4](#)). However, proxy evidence suggests that AMOC had already slowed and that North Atlantic SSTs were already cold before ice-rafted debris (IRD) deposition, challenging this view ([2](#)). Reconstructing event phasing across different proxy records is hampered by the difficulty in dating Heinrich sediment deposits ([1](#)). As of yet, the intrastadial timings of individual Heinrich events have not been well determined, and estimates of individual event duration vary by an order of magnitude ([1](#)). The sequence and phasing of millennial-scale climate phenomena appear to be intrinsically linked to the initiation of deglaciation ([5](#)), providing additional impetus for investigation.

Here we present a precise, highly resolved record of atmospheric methane (CH_4) concentrations, determined by a recently developed continuous measurement technique ([6](#)), for the Last Glacial Period and the deglacial transition from the West Antarctic Ice Sheet (WAIS) Divide (WD) ice core ([Fig. 1](#)). Ice core CH_4 is a globally integrated signal, primarily reflecting the response of the terrestrial biosphere, predominantly wetlands, to hydroclimatic change ([7](#)). The WD trace gas record is especially appropriate for paleoreconstruction because rapid occlusion of air bubbles in the firn column results in minimal smoothing of atmospheric signals (estimated gas age distribution width 20 to 50 years, [fig. S1](#)). The sampling resolution of our CH_4 record varies between 0.5 and 13 years, meaning that all climate-driven CH_4 signals preserved in the ice are captured ([8](#)). Continuous CH_4 analysis produces measurements with excellent internal precision [$\leq \pm 0.5$ parts per billion (ppb), 2σ] that are reproducible to within ± 3 ppb (2σ) over intervals of days to weeks ([table S1](#)).

- [Download high-res image](#)

- [Open in new tab](#)
- [Download Powerpoint](#)

Fig. 1WD continuous CH₄ and other environmental proxies.

(A) WD CH₄ growth rates between -1 to 1 ppb year⁻¹ (dark green) and growth rates exceeding these bounds (light green), plotted with vertical gray lines marking interstadial onsets; (B) CH₄ 2-year spline fit (red) (8) on the WD2014 time scale; (C) North Greenland Ice Core Project (NGRIP) δ¹⁸O_{ice} 20-year mean record (five-point running mean, dark blue) (27) on a modified Greenland Ice Core Chronology 2005 time scale (8); (D) Hulu cave (China) δ¹⁸O_{calcite} from speleothems: H82 (black) (28), MSD (light gray) and MSL (dark gray) (10) (note inverted y axis); (E) Pacupahuain (Peru) speleothem δ¹⁸O_{calcite} (three-point running mean, dark purple) (29); and (F) Ca/Sr, an indicator of detrital carbonate, from marine sediment core U1208 (reoccupied Deep Sea Drilling Project site 609) (30) and IRD stack of North Atlantic sediment cores (arbitrary units multiplied by 300) (26). HSs 1 to 6 are shaded: pale yellow-shaded HSs contain Heinrich events sourced from the Hudson Strait (high Ca/Sr) and pale blue-shaded HSs contain Heinrich events with a different (or mixed) provenance. Even-numbered DO cycles and the Bølling/Allerød (B/A) and Younger Dryas (YD) intervals are indicated. VSMOW, Vienna standard mean ocean water; VPDB, Vienna Bee Dee belemnite standard.

Our continuous CH₄ record spanning 67.2 to 9.8 thousand years before the present (ky B.P.) (present = 1950 CE) (Fig. 1) resolves growth rates that exceed maximum values previously reported for abrupt climate transitions in this time period (9), the fastest rate occurring at the Younger Dryas termination (>6 ppb year⁻¹). These are minimum estimates of atmospheric growth rate, because firn-related smoothing processes may have attenuated rapid atmospheric CH₄ changes. We observe no systematic decrease in CH₄ growth rate across successive DO interstadial onsets (9); however, CH₄ growth from stadial to interstadial is significantly faster than decay back to stadial levels.

WD CH₄ covaries with Greenland δ¹⁸O_{ice} and Hulu cave δ¹⁸O_{calcite} at millennial to centennial time scales (Fig. 1). The close correspondence of these records can be related to latitudinal shifts in the Intertropical Convergence Zone (ITCZ) and its terrestrial component, which we refer to as tropical rain belts; during warm interstadials, the tropical rain belts migrate northward, intensifying Northern Hemisphere monsoonal rainfall and wetland CH₄ production, whereas the reverse occurs in cool stadials (7, 10). Southern Hemisphere monsoonal strength proxies show an antiphase relationship across DO cycles: relatively wet during stadials and dry during interstadials (Fig. 1E). However, these relationships break down within HSs 1, 2, 4, and 5.

In each case, the early HS is characterized by relatively low CH₄ concentrations, and the late HS commences with an abrupt 32 to 53 ppb

CH₄ increase (**Fig. 2**), which occurs at growth rates comparable to those of DO interstadial onsets (**Fig. 1A**). Within late HSs 4 and 5, CH₄ concentrations overshoot before returning to a stable level after ~ 90 and 160 years, respectively (**Fig. 2**). No overshoot associated with the abrupt CH₄ increase within HS 2 (24.03 ky B.P.) is resolved, possibly due to inadequate sampling resolution through this section (**Fig. 2**). The Greenland ice core temperature proxy $\delta^{15}\text{N}$ of N₂ indicates clearly that this abrupt CH₄ increase is not associated with DO 2, which occurred >750 years later (fig. S7). CH₄ concentrations are steadily rising throughout HS 1 as a result of deglaciation, but an abrupt increase of 32 ppb is resolved at 16.15 ky B.P. (**11**). CH₄ levels return to the underlying trend within ~190 years. All late HS phases are characterized by elevated CH₄ concentrations, relative to early HS phases, that persist until the following DO event (**Fig. 2**). No similar anomalous CH₄ signals are observed within other stadials, including HSs 3, 5a, and 6 (fig. S3).

- [Download high-res image](#)
- [Open in new tab](#)
- [Download Powerpoint](#)

Fig. 2 Detailed view of HSs 1, 2, 4, and 5.

Abrupt CH₄ increases (**A**) linked to the onset of Heinrich events are observed within HSs 1, 2, 4, and 5. Discrete CH₄ measurements (brown symbols) used to construct the CH₄ 2-year spline fit [red, (**8**)] within HS 2 are displayed. HSs are divided into early HSs (green shading), before the abrupt CH₄ increase (left-hand vertical line), and late HSs (yellow shading). NGRIP (Greenland) $\delta^{18}\text{O}_{\text{ice}}$ (**27**) [(**B**), five-point running mean, dark blue] shows no abrupt temperature signal in HSs 1, 2, 4, and 5. Hulu (China) $\delta^{18}\text{O}_{\text{calcite}}$ (**10, 28**) (**C**) suggests weakening of the East Asian monsoon, whereas growth phases of speleothems from northeastern Brazil (**31**) [(**D**), purple diamonds] suggest strengthening of the South American summer monsoon. U-Th age control points for Hulu speleothems are displayed for HSs 2, 4, and 5 (black/gray diamonds) with 2 σ uncertainties. Age control points for HS1 are too numerous to display. A stack of IRD records from North Atlantic sediment cores is displayed [(**E**), purple] with upper (pale blue) and lower (dark blue) 95% confidence intervals in age model (**26**). Late HSs durations, suggested as maximum durations for the climatic impacts of Heinrich events, are indicated with 2 σ uncertainty estimates (**8**). Yellow shading is extended upward to highlight speleothem signals with timings coincident with late HSs 1 and 2.

The abrupt CH₄ signals within HSs 1, 2, 4, and 5 are comparable in magnitude and rate to DO interstadial onsets (**Fig. 1A**), and yet CH₄ appears

to be completely decoupled from Greenland $\delta^{18}\text{O}_{\text{ice}}$ (**Fig. 2**) and $\delta^{15}\text{N}$ (**12**). Neither temperature proxy shows the complementary abrupt increases characteristic of interstadials. Furthermore, the CH_4 signals of HSs 1, 2, 4, and 5 are associated with isotopic enrichment of Hulu $\delta^{18}\text{O}_{\text{calcite}}$ (**Fig. 2**) rather than depletion, indicating reduction in the strength of the East Asian monsoon (**10**). The excess CH_4 within late HSs 1, 2, 4, and 5 must therefore result from fundamentally different climatic conditions than interstadial CH_4 .

Other paleoclimate proxies from the Arabian Sea (**13**), northern Africa (**14**), and Borneo (**15**) provide evidence for anomalously dry conditions across the Northern Hemisphere during HSs. Furthermore, South American speleothems (**Figs. 1** and **2**), Australian sediment archives (**16**), and ice core $\delta^{18}\text{O}_{\text{atm}}$ data (**17**) (fig. S8) suggest concurrent intensification of precipitation across the Southern Hemisphere tropics and subtropics during these intervals. Taken together, the paleoclimatic evidence suggests that the ITCZ occupied an extreme southerly location during HSs. Absolute dates on the Hulu speleothem in HSs 1 and 2, and speleothems from NE Brazil in HS 1 only, indicate that this southerly shift occurred abruptly partway through the stadial, as the anomalous CH_4 signals do (**Fig. 2**). Southerly ITCZ displacement can occur in response to Northern Hemisphere cooling and sea-ice expansion (**18**) and is a consistent outcome of freshwater hosing experiments (**19, 20**) designed to simulate the effects of iceberg discharge.

This leads us to hypothesize that extended sea-ice cover and associated cold air temperatures in the north, resulting from Heinrich events (**1**), severely restricted the northerly seasonal migration of the tropical rain belts, forcing them to reside at southerly latitudes for longer periods during their seasonal evolution, thereby extending and intensifying the wet season across the Southern Hemisphere. A similar change in precipitation seasonality across South America has been observed in response to an extreme freshwater hosing experiment (**20**). If the resultant gain in Southern Hemisphere tropical wetlands were to exceed the loss in the north, a net gain of CH_4 -producing wetland would result. The excess stadial CH_4 we observe could therefore have been sourced from the Southern Hemisphere, as speculated for individual events (**11, 21**).

A first-order comparison of WD CH_4 and Greenland CH_4 data (**9**) suggests that little change in the CH_4 inter-polar difference occurred between early and late HSs 4 and 5, supporting our hypothesized tropical source for the additional CH_4 . Ice core CH_4 isotopic data may also indicate an increased contribution of Southern Hemisphere wetlands to the CH_4 budget during late HS 4 (**21**).

To explore our idea quantitatively, we use a heuristic approach in which the modern-day seasonal distribution of tropical (40°S to 40°N) land rainfall is modified in an idealized manner. We adopt an intense precipitation threshold [monthly average $>5 \text{ mm day}^{-1}$ (**8**)] as indicative of potential wetland presence. We highlight that potential wetland area peaks twice a year using

this metric, once during the summer (monsoon season) of each hemisphere (**Fig. 3A**), which is similar to the seasonal distribution of tropical CH₄ emissions (**22**). The land rainfall distribution is modified by incrementally reducing the intensity of the boreal summer land rainfall peak and redistributing that rainfall, forcing it to occupy more southerly latitudes during the transitional seasons (fig. S5) (**8**).

- [Download high-res image](#)
- [Open in new tab](#)
- [Download Powerpoint](#)

Fig. 3

Effect of increased Southern Hemisphere weighting of tropical rainfall seasonality on intense land rainfall distribution. (A) Monthly distribution of the percent of land area with intense (monthly average >5 mm day⁻¹) rainfall within 40°S to 40°N. Modern-day monthly distribution peaks twice a year, once in the summer of each hemisphere (black). The effect of modifying rainfall seasonality on this distribution is shown. Rainfall seasonality becomes increasingly Southern Hemisphere-weighted by incrementally reducing the intensity of the boreal summer land rainfall peak, from 100% (black) to 90% (blue), 80% (light blue), 70% (dark green), 60% (light green), and 50% (orange), with the austral summer rainfall peak held fixed (**8**). (B) Annual mean percent of land area with intense rainfall for the same increments of the boreal summer land rainfall peak amplitude.

As the boreal summer rainfall maximum is progressively reduced, the land area with intense rainfall in boreal summer decreases (**Fig. 3A**), as does the annual average of land area with intense rainfall (**Fig. 3B**). This is consistent with colder stadials having lower CH₄ concentrations, as observed (**Fig. 1**). A minimum in the annual average land area with intense rainfall is reached at ~60% of the boreal summer rainfall peak amplitude, corresponding to an ~7% total loss of potential wetland area. Crucially, a further reduction of boreal summer rainfall causes a relative increase in potential wetland area of 400,400 km² as compared to the minimum (**Fig. 3B**), primarily during October and November (**Fig. 3A**).

Assuming that all of this additional land is indeed wetland, the increase can be roughly approximated to an increase in CH₄ emissions of 29 Tg year⁻¹ (**8**). This outcome should be treated with caution because, although rainfall is a powerful control on tropical wetland CH₄ emissions, several other factors, which we do not account for, influence wetland formation and/or CH₄ emissions (**23**). However, our ice core CH₄ data show a similar magnitude of CH₄ emissions rate increase (6.5 to 21.2 Tg year⁻¹) between early and late

HS phases (8), supporting our approach. This scenario provides a simple, heuristic explanation for the observations, but more complex changes in rainfall distribution, not captured by our seasonal modification, probably occurred. For example, warmer Southern Hemisphere temperatures may have caused southward movement of the austral summer rainfall peak (24), whereas we assume an unaltered austral summer rainfall peak. We have not adopted a coupled climate-biogeochemistry modeling approach because it is not yet clear how to effectively represent a regular Greenlandic stadial versus a Heinrich stadial; the different processes occurring in the North Atlantic are not adequately understood.

Given the framework outlined above—increased Southern Hemisphere CH₄ production in response to Northern Hemisphere cooling caused by a Heinrich event—and given that the atmospheric reorganization can occur within a decade (18), we propose timings for the first impacts of Heinrich events on tropical hydroclimate, which could closely correspond to the initiation of the Heinrich events themselves. The CH₄ increases we ascribe to Heinrich events 1, 2, 4, and 5 are dated as 16.13 ± 0.12 ky B.P., 24.03 ± 0.37 ky B.P., 39.54 ± 0.38 ky B.P. and 48.39 ± 0.38 ky B.P., respectively, in the WD2014 chronology (25) [2σ uncertainty (8)]. Our proposed ages for Heinrich events 1 and 2 match the timing of maximum IRD observed in a stack of North Atlantic sediment records (26) (Fig. 2), and closely correspond to calibrated ¹⁴C-based estimates (1). Despite these encouraging signs, we cannot be certain of the phasing of events. For example, the scenario of Northern Hemisphere cooling leading to CH₄ increase that we describe could potentially occur before the Heinrich event, maybe even triggering the event. This seems an unlikely possibility, given the requirement for another forcing mechanism, the abrupt nature of the CH₄ signals, and their unique occurrence in Heinrich stadials, but it cannot be ruled out.

The direct impact of a Heinrich event must cease once the ensuing interstadial commences and Northern Hemisphere climate warms (Fig. 1). We calculated maximum durations for the climatic impact of individual Heinrich events, perhaps largely on tropical hydrology, as ranging from 740 to 1520 years (Fig. 2). These estimates are significantly higher than the best guess for the duration of the actual iceberg armada (1 to 500 years) (1). We therefore suggest that this duration is related to a prolonged state of severely slowed or collapsed AMOC, maintained by extensive North Atlantic sea ice. This does not preclude the likelihood that AMOC was already relatively weak before Heinrich events, but rather explains why AMOC strength remained low through an extended stadial period when most coupled models suggest recovery of the overturning circulation within a few hundred years (19). The late HS plateaus in CH₄ concentration, particularly in HSs 4 and 5, are remarkably stable in comparison to interstadials (Fig. 1), suggesting limited variability in tropical precipitation and a relatively stable

AMOC state. It is tempting to speculate on whether we capture information about the actual iceberg armada duration in the ~90- to 190-year CH₄ overshoots resolved during HSs 1, 4, and 5 (**Fig. 2**). However, short-duration CH₄ overshoots are not unique to these events and are in fact a feature of nearly all interstadial onsets, possibly resulting from an intrinsic response of the atmospheric system to rapid reorganization or intensive methanogenesis in newly inundated wetlands.

We suggest that our results provide motivation for climate modeling experiments to further investigate the difference between regular stadials and Heinrich stadials in the North Atlantic region and their respective impacts on tropical climate. Moreover, it is intriguing that only Heinrich events 1, 2, 4, and 5 are associated with Southern Hemisphere CH₄ signals. These four Heinrich events have relatively thick and spatially extensive sediment deposits, rich in detrital carbonate (**Fig. 1**) sourced from the Hudson Strait, and are linked to surging of the Laurentide ice sheet (**1**). Were the remaining Heinrich events too insignificant in scale to greatly perturb tropical climate, or did they not influence the same climate-sensitive location?

Supplementary Materials

www.sciencemag.org/content/348/6238/1016/suppl/DC1

Materials and Methods

Supplementary Text

Figs. S1 to S8

Tables S1 and S2

References (**32–53**)

References and Notes

1. [↩](#)

1. S. R. Hemming

, Heinrich events: Massive late Pleistocene detritus layers of the North Atlantic and their global climate imprint. *Rev. Geophys.* **42**, RG1005 (2004). doi:10.1029/2003RG000128

UNIVERSITY OF CALIFORNIA

BERKELEY
Library

UC-eLinksCrossRefGoogle Scholar

2. [↩](#)

P. U. Clark, S. W. Hostetler, N. G. Pisias, A. Schmittner, K. J. Meissner, in *Geophysical Monograph Series*, A. Schmittner, J. C. H. Chiang, S. R. Hemming, Eds. (American Geophysical Union, Washington, DC, 2007), vol. 173, pp. 209–246.

[Google Scholar](#)

3. [↩](#)

1. G. Bond,
2. W. Broecker,
3. S. Johnsen,
4. J. McManus,
5. L. Labeyrie,
6. J. Jouzel,
7. G. Bonani

, Correlations between climate records from North Atlantic sediments and Greenland ice. *Nature* **365**, 143–147 (1993).doi:10.1038/365143a0

ACCESS PROVIDED BY

 BERKELEY
Library
UNIVERSITY OF CALIFORNIA

[UC-eLinks](#)[CrossRef](#)[Web of Science](#)[Google Scholar](#)

4. [↩](#)

1. W. S. Broecker

, Massive iceberg discharges as triggers for global climate change. *Nature* **372**, 421–424(1994). doi:10.1038/372421a0

ACCESS PROVIDED BY

 BERKELEY
Library
UNIVERSITY OF CALIFORNIA

[UC-eLinks](#)[CrossRef](#)[Web of Science](#)[Google Scholar](#)

5. [↩](#)

1. E. W. Wolff,
2. H. Fischer,
3. R. Röthlisberger

, Glacial terminations as southern warmings without northern control. *Nat. Geosci.* **2**, 206–209 (2009). doi:10.1038/ngeo442

ACCESS PROVIDED BY

 BERKELEY
Library
UNIVERSITY OF CALIFORNIA

[UC-eLinks](#)[CrossRef](#)[Google Scholar](#)

6. [↩](#)

1. R. H. Rhodes,
2. X. Faïn,
3. C. Stowasser,
4. T. Blunier,
5. J. Chappellaz,
6. J. R. McConnell,
7. D. Romanini,
8. L. E. Mitchell,
9. E. J. Brook


, Continuous methane measurements from a late Holocene Greenland ice core: Atmospheric and in-situ signals. *Earth Planet. Sci. Lett.* **368**, 9–19 (2013). doi:10.1016/j.epsl.2013.02.034

ACCESSible BY
 [UC-eLinks](#)[CrossRef](#)[Google Scholar](#)

7. [↩](#)

1. E. J. Brook,
2. S. Harder,
3. J. Severinghaus,
4. E. J. Steig,
5. C. M. Sucher

, On the origin and timing of rapid changes in atmospheric methane during the Last Glacial Period. *Global Biogeochem. Cycles* **14**, 559–572(2000). doi:10.1029/1999GB001182

ACCESSible BY
 [UC-eLinks](#)[CrossRef](#)[Web of Science](#)[Google Scholar](#)

8. [↩](#) Materials and methods are available as supplementary materials on *Science Online*.

9. [↩](#)

1. J. Chappellaz,
2. C. Stowasser,
3. T. Blunier,
4. D. Baslev-Clausen,
5. E. J. Brook,

6. R. Dallmayr,
7. X. Fain,
8. J. E. Lee,
9. L. E. Mitchell,
10. O. Pascual,
11. D. Romanini,
12. J. Rosen,
13. S. Schüpbach


, High-resolution glacial and deglacial record of atmospheric methane by continuous-flow and laser spectrometer analysis along the NEEM ice core. *Clim. Past* **9**, 2579–2593 (2013). doi:10.5194/cp-9-2579-2013

ACCESS FULL BY
 [UC-eLinks](#)[CrossRef](#)[Google Scholar](#)

10. [↩](#)

1. Y. J. Wang,
2. H. Cheng,
3. R. L. Edwards,
4. Z. S. An,
5. J. Y. Wu,
6. C. C. Shen,
7. J. A. Dorale

, A high-resolution absolute-dated late Pleistocene Monsoon record from Hulu Cave, China. *Science* **294**, 2345–2348 (2001).doi:10.1126/science.1064618 pmid:11743199

ACCESS FULL BY
 [UC-eLinks](#)[Abstract/FREE Full Text](#)[Google Scholar](#)

11. [↩](#)

1. S. A. Marcott,
2. T. K. Bauska,
3. C. Buizert,
4. E. J. Steig,
5. J. L. Rosen,
6. K. M. Cuffey,

7. T. J. Fudge,
8. J. P. Severinghaus,
9. J. Ahn,
10. M. L. Kalk,
11. J. R. McConnell,
12. T. Sowers,
13. K. C. Taylor,
14. J. W. White,
15. E. J. Brook


, Centennial-scale changes in the global carbon cycle during the last deglaciation. *Nature* **514**, 616–619 (2014). doi:10.1038/nature13799 p mid:25355363

ACCESSible BY
 [UC-eLinks](#) [CrossRef](#) [PubMed](#) [Google Scholar](#)

12. [↵](#)

1. P. Kindler,
2. M. Guillevic,
3. M. Baumgartner,
4. J. Schwander,
5. A. Landais,
6. M. Leuenberger,
7. R. Spahni,
8. E. Capron,
9. J. Chappellaz

, Temperature reconstruction from 10 to 120 kyr b2k from the NGRIP ice core. *Clim. Past* **10**, 887–902 (2014). doi:10.5194/cp-10-887-2014

ACCESSible BY
 [UC-eLinks](#) [CrossRef](#) [Web of Science](#) [Google Scholar](#)

13. [↵](#)

1. G. Deplazes,
2. A. Lückge,
3. L. C. Peterson,
4. A. Timmermann,

5. Y. Hamann,
6. K. A. Hughen,
7. U. Röhl,
8. C. Laj,
9. M. A. Cane,
10. D. M. Sigman,
11. G. H. Haug

, Links between tropical rainfall and North Atlantic climate during the last glacial period. *Nat. Geosci.* **6**, 213–217 (2013). doi:10.1038/ngeo1712

ACCESS PROVIDED BY
 [UC-eLinks](#) [CrossRef](#) [Google Scholar](#)

14. [↩](#)

1. J. A. Collins,
2. A. Govin,
3. S. Mulitza,
4. D. Heslop,
5. M. Zabel,
6. J. Hartmann,
7. U. Röhl,
8. G. Wefer

, Abrupt shifts of the Sahara–Sahel boundary during Heinrich stadials. *Clim. Past* **9**, 1181–1191 (2013). doi:10.5194/cp-9-1181-2013

ACCESS PROVIDED BY
 [UC-eLinks](#) [CrossRef](#) [Google Scholar](#)

15. [↩](#)

1. S. A. Carolin,
2. K. M. Cobb,
3. J. F. Adkins,
4. B. Clark,
5. J. L. Conroy,
6. S. Lejau,
7. J. Malang,

8. A. A. Tuen
, Varied response of western Pacific hydrology to climate forcings over the last glacial period. *Science* **340**, 1564-1566 (2013). doi:10.1126/science.1233797 pmid:23744779

ACCESS PROVIDED BY



[UC-eLinks](#)[Abstract/FREE Full Text](#)[Google Scholar](#)

16. [↩](#)

1. J. Muller,
2. M. Kylander,
3. R. A. J. Wüst,
4. D. Weiss,
5. A. Martinez-Cortizas,
6. A. N. LeGrande,
7. T. Jennerjahn,
8. H. Behling,
9. W. T. Anderson,
10. G. Jacobson

, Possible evidence for wet Heinrich phases in tropical NE Australia: The Lynch's Crater deposit. *Quat. Sci. Rev.* **27**, 468-475 (2008). doi:10.1016/j.quascirev.2007.11.006

ACCESS PROVIDED BY



[UC-eLinks](#)[CrossRef](#)[Web of Science](#)[Google Scholar](#)

17. [↩](#)

1. J. P. Severinghaus,
2. R. Beaudette,
3. M. A. Headly,
4. K. Taylor,
5. E. J. Brook

, Oxygen-18 of O₂ records the impact of abrupt climate change on the terrestrial biosphere. *Science* **324**, 1431-1434 (2009). doi:10.1126/science.1169473 pmid:19520957

ACCESS PROVIDED BY



[UC-eLinks](#)[Abstract/FREE Full Text](#)[Google Scholar](#)

18. [↩](#)

1. J. C. H. Chiang,
2. C. M. Bitz

, Influence of high latitude ice cover on the marine intertropical convergence zone. *Clim. Dyn.* **25**, 477–496 (2005). doi:10.1007/s00382-005-0040-5

ACCESS FULL BY



[UC-eLinks](#)[CrossRef](#)[Web of Science](#)[Google Scholar](#)

19. [↩](#)

1. M. Kageyama,
2. U. Merkel,
3. B. Otto-Bliesner,
4. M. Prange,
5. A. Abe-Ouchi,
6. G. Lohmann,
7. R. Ohgaito,
8. D. M. Roche,
9. J. Singarayer,
10. D. Swingedouw,
11. X Zhang

, Climatic impacts of fresh water hosing under Last Glacial Maximum conditions: A multi-model study. *Clim. Past* **9**, 935–953 (2013). doi:10.5194/cp-9-935-2013

ACCESS FULL BY



[UC-eLinks](#)[CrossRef](#)[Web of Science](#)[Google Scholar](#)

20. [↩](#)

1. L. A. Parsons,
2. J. Yin,
3. J. T. Overpeck,
4. R. J. Stouffer,
5. S. Malyshev

, Influence of the Atlantic Meridional Overturning Circulation on the monsoon rainfall and carbon balance of the American tropics. *Geophys. Res. Lett.* **41**, 2013GL058454 (2014).

21. [↵](#)

1. M. Guillevic,
2. L. Bazin,
3. A. Landais,
4. C. Stowasser,
5. V. Masson-Delmotte,
6. T. Blunier,
7. F. Eynaud,
8. S. Falourd,
9. E. Michel,
10. B. Minster,
11. T. Popp,
12. F. Prié,
13. B. M. Vinther

, Evidence for a three-phase sequence during Heinrich Stadial 4 using a multiproxy approach based on Greenland ice core records. *Clim. Past* **10**, 2115–2133(2014). doi:10.5194/cp-10-2115-2014

22. [↵](#)

1. P. Bergamaschi,
2. C. Frankenberg,
3. J. F. Meirink,
4. M. Krol,
5. M. G. Villani,
6. S. Houweling,
7. F. Dentener,
8. E. J. Dlugokencky,
9. J. B. Miller,
10. L. V. Gatti,

11. A. Engel,

12. I. Levin

, Inverse modeling of global and regional CH₄ emissions using
SCIAMACHY satellite retrievals. J. Geophys. Res.
Atmos. **114**, D22301 (2009).doi:10.1029/2009JD012287

ACCESS FULL BY

Library

[UC-eLinks](#)[CrossRef](#)[Google Scholar](#)

23. [↶](#)

1. B. P. Walter,

2. M. Heimann,

3. E. Matthews

, Modeling modern methane emissions from natural wetlands: 2.
Interannual variations 1982–1993. J. Geophys. Res.
Atmos. **106**, 34207–34219 (2001).doi:10.1029/2001JD900164

ACCESS FULL BY

Library

[UC-eLinks](#)[CrossRef](#)[Google Scholar](#)

24. [↶](#)

1. I. Cvijanovic,

2. P. L. Langen,

3. E. Kaas,

4. P. D. Ditlevsen

, Southward intertropical convergence zone shifts and implications for
an atmospheric bipolar seesaw. J. Clim. **26**, 4121–
4137 (2013). doi:10.1175/JCLI-D-12-00279.1

ACCESS FULL BY

Library

[UC-eLinks](#)[CrossRef](#)[Google Scholar](#)

25. [↶](#)

1. C. Buizert,

2. K. M. Cuffey,

3. J. P. Severinghaus,

4. D. Baggenstos,

5. T. J. Fudge,

6. E. J. Steig,

7. B. R. Markle,

8. M. Winstrup,
9. R. H. Rhodes,
10. E. J. Brook,
11. T. A. Sowers,
12. G. D. Clow,
13. H. Cheng,
14. R. L. Edwards,
15. M. Sigl,
16. J. R. McConnell,
17. K. C. Taylor

, The WAIS Divide deep ice core WD2014 chronology – Part 1: Methane synchronization (68–31 ka BP) and the gas age–ice age difference. *Clim. Past* **11**, 153–173 (2015). doi:10.5194/cp-11-153-2015

 [UC-eLinks](#) [CrossRef](#) [Google Scholar](#)

26. [↩](#)

1. J. V. Stern,
2. L. E. Lisiecki

, North Atlantic circulation and reservoir age changes over the past 41,000 years. *Geophys. Res. Lett.* **40**, 3693–3697 (2013). doi:10.1002/grl.50679

 [UC-eLinks](#) [CrossRef](#) [Google Scholar](#)

27. [↩](#)

1. A. Svensson,
2. K. K. Andersen,
3. M. Bigler,
4. H. B. Clausen,
5. D. Dahl-Jensen,
6. S. M. Davies,
7. S. J. Johnsen,
8. R. Muscheler,
9. F. Parrenin,

10. S. O. Rasmussen,
11. R. Röthlisberger,
12. I. Seierstad,
13. J. P. Steffensen,
14. B. M. Vinther

, A 60,000 year Greenland stratigraphic ice core chronology. *Clim. Past* **4**, 47-57 (2008). doi:10.5194/cp-4-47-2008

Accessed by



[UC-eLinks](#)[CrossRef](#)[Web of Science](#)[Google Scholar](#)

28. [↵](#)

1. J. Southon,
2. A. L. Noronha,
3. H. Cheng,
4. R. L. Edwards,
5. Y. Wang

, A high-resolution record of atmospheric ¹⁴C based on Hulu Cave speleothem H82. *Quat. Sci. Rev.* **33**, 32-41 (2012).doi:10.1016/j.quascirev.2011.11.022

Accessed by



[UC-eLinks](#)[CrossRef](#)[Web of Science](#)[Google Scholar](#)

29. [↵](#)

1. L. C. Kanner,
2. S. J. Burns,
3. H. Cheng,
4. R. L. Edwards

, High-latitude forcing of the South American summer monsoon during the Last Glacial. *Science* **335**, 570-573 (2012). doi:10.1126/science.1213397pmid:22245741

Accessed by



[UC-eLinks](#)[Abstract/FREE Full Text](#)[Google Scholar](#)

30. [↵](#)

1. D. A. Hodell,
2. J. E. Channell,

3. J. H. Curtis,
4. O. E. Romero,
5. U. Röhl

, Onset of “Hudson Strait” Heinrich events in the eastern North Atlantic at the end of the middle Pleistocene transition (640 ka)? *Paleoceanography* **23**, PA4218 (2008). doi:10.1029/2008PA001591

ACCESS PROVIDED BY
 [UC-eLinks](#)[CrossRef](#)[Google Scholar](#)

31. [↩](#)

1. X. Wang,
2. A. S. Auler,
3. R. L. Edwards,
4. H. Cheng,
5. P. S. Cristalli,
6. P. L. Smart,
7. D. A. Richards,
8. C. C. Shen

, Wet periods in northeastern Brazil over the past 210 kyr linked to distant climate anomalies. *Nature* **432**, 740–743 (2004). doi:10.1038/nature03067 pmid:15592409

ACCESS PROVIDED BY
 [UC-eLinks](#)[CrossRef](#)[PubMed](#)[Web of Science](#)[Google Scholar](#)

32. [↩](#)

1. J. L. Rosen,
2. E. J. Brook,
3. J. P. Severinghaus,
4. T. Blunier,
5. L. E. Mitchell,
6. J. E. Lee,
7. J. S. Edwards,
8. V. Gkinis

, An ice core record of near-synchronous global climate changes at the Bølling transition. *Nat. Geosci.* **7**, 459–463 (2014). doi:10.1038/ngeo2147

33.

1. C. Stowasser,
2. C. Buizert,
3. V. Gkinis,
4. J. Chappellaz,
5. S. Schüpbach,
6. M. Bigler,
7. X. Faïn,
8. P. Sperlich,
9. M. Baumgartner,
10. A. Schilt,
11. T. Blunier

, Continuous measurements of methane mixing ratios from ice cores. *Atmospheric Meas. Tech.* **5**, 999–1013 (2012). doi:10.5194/amt-5-999-2012

34.

1. D. Romanini,
2. M. Chenevier,
3. S. Kassi,
4. M. Schmidt,
5. C. Valant,
6. M. Ramonet,
7. J. Lopez,
8. H.-J. Jost

, Optical-feedback cavity-enhanced absorption: A compact spectrometer for real-time measurement of atmospheric methane. *Appl. Phys. B* **83**, 659–667 (2006). doi:10.1007/s00340-006-2177-2

35. Optical feedback cavity enhanced absorption spectroscopy technology is now commercialized for industrial applications by AP2E, France.

[Google Scholar](#)

36.

1. E. J. Dlugokencky

, Conversion of NOAA atmospheric dry air CH₄ mole fractions to a gravimetrically prepared standard scale. J. Geophys. Res. **110**, D18306 (2005). doi:10.1029/2005JD006035

ACCESS FULL BY

Library

[UC-eLinks](#)[CrossRef](#)[Google Scholar](#)

37.

1. L. E. Mitchell,

2. E. J. Brook,

3. T. Sowers,

4. J. R. McConnell,

5. K. Taylor

, Multidecadal variability of atmospheric methane, 1000-1800 C.E. J. Geophys. Res. **116**, G02007 (2011). doi:10.1029/2010JG001441

ACCESS FULL BY

Library

[UC-eLinks](#)[CrossRef](#)[Google Scholar](#)

38.

1. D. Allan

, Statistics of atomic frequency standards. Proc. Inst. Electr. Electron. Eng. **54**, 221-230 (1966).doi:10.1109/PROC.1966.4634

ACCESS FULL BY

Library

[UC-eLinks](#)[CrossRef](#)[Google Scholar](#)

39.

1. J. Schwander,

2. J.-M. Barnola,

3. C. Andri ,

4. M. Leuenberger,

5. A. Ludin,

6. D. Raynaud,
7. B. Stauffer


, The age of the air in the firn and the ice at Summit, Greenland. J. Geophys. Res. **98**, 2831–2838 (1993).doi:10.1029/92JD02383

 [UC-eLinks](#)[CrossRef](#)[Google Scholar](#)

40.

1. G. J. Huffman,
2. D. T. Bolvin,
3. E. J. Nelkin,
4. D. B. Wolff,
5. R. F. Adler,
6. G. Gu,
7. Y. Hong,
8. K. P. Bowman,
9. E. F. Stocker

,The TRMM Multisatellite Precipitation Analysis (TMPA): Quasi-global, multiyear, combined-sensor precipitation estimates at fine scales. J. Hydrometeorol. **8**, 38–55 (2007). doi:10.1175/JHM560.1

 [UC-eLinks](#)[CrossRef](#)[Web of Science](#)[Google Scholar](#)

41.

1. M. Baumgartner,
2. A. Schilt,
3. O. Eicher,
4. J. Schmitt,
5. J. Schwander,
6. R. Spahni,
7. H. Fischer,
8. T. F. Stocker

, High-resolution inter-polar difference of atmospheric methane around the Last Glacial Maximum. Biogeosciences **9**, 3961–3977 (2012). doi:10.5194/bg-9-3961-2012

42.

1. D. T. Shindell,
2. B. P. Walter,
3. G. Faluvegi

, Impacts of climate change on methane emissions from wetlands. *Geophys. Res. Lett.* **31**, L21202 (2004). doi:10.1029/2004GL021009

Let. **31**, L21202 (2004). doi:10.1029/2004GL021009

43. Data Announcement 88-MGG-02, *Digital Relief of the Surface of the Earth* (National Geophysical Data Center, National Oceanic and Atmospheric Administration, Boulder, CO, 1988).

[Google Scholar](#)

44.

1. M. Cao,
2. S. Marshall,
3. K. Gregson

, Global carbon exchange and methane emissions from natural wetlands: Application of a process-based model. *J. Geophys. Res.* **101**, 14399 (1996). doi:10.1029/96JD00219

Res. **101**, 14399 (1996). doi:10.1029/96JD00219

45.

1. J. R. Melton,
2. R. Wania,
3. E. L. Hodson,
4. B. Poulter,
5. B. Ringeval,
6. R. Spahni,
7. T. Bohn,
8. C. A. Avis,

9. D. J. Beerling,
10. G.Chen,
11. A. V. Eliseev,
12. S. N. Denisov,
13. P. O. Hopcroft,
14. D. P. Lettenmaier,
15. W. J. Riley,
16. J. S. Singarayer,
17. Z. M. Subin,
18. H. Tian,
19. S. Zürcher,
20. V. Brovkin,
21. P. M. van Bodegom,
22. T. Kleinen,
23. Z. C. Yu,
24. J. O. Kaplan

, Present state of global wetland extent and wetland methane modelling: Conclusions from a model inter-comparison project (WETCHIMP). *Biogeosciences* **10**, 753–788 (2013). doi:10.5194/bg-10-753-2013

ACCESSible BY



[UC-eLinks](#)[CrossRef](#)[Web of Science](#)[Google Scholar](#)

46.

1. P. O. Hopcroft,
2. P. J. Valdes,
3. R. Wania,
4. D. J. Beerling

, Limited response of peatland CH₄ emissions to abrupt Atlantic Ocean circulation changes in glacial climates. *Clim. Past* **10**, 137–154 (2014). doi:10.5194/cp-10-137-2014

ACCESSible BY



[UC-eLinks](#)[CrossRef](#)[Google Scholar](#)

47.

1. P. O. Hopcroft,

2. P. J. Valdes,
3. D. J. Beerling

, Simulating idealized Dansgaard-Oeschger events and their potential impacts on the global methane cycle. *Quat. Sci. Rev.* **30**, 3258–3268 (2011). doi:10.1016/j.quascirev.2011.08.012

ACCESSible BY



[UC-eLinks](#)[CrossRef](#)[Google Scholar](#)

48.

1. J. G. Levine,
2. E. W. Wolff,
3. P. O. Hopcroft,
4. P. J. Valdes

, Controls on the tropospheric oxidizing capacity during an idealized Dansgaard-Oeschger event, and their implications for the rapid rises in atmospheric methane during the last glacial period. *Geophys. Res. Lett.* **39**, L12805 (2012). doi:10.1029/2012GL051866

ACCESSible BY



[UC-eLinks](#)[CrossRef](#)[Google Scholar](#)

49.

1. J. G. Levine,
2. E. W. Wolff,
3. A. E. Jones,
4. L. C. Sime,
5. P. J. Valdes,
6. A. T. Archibald,
7. G. D. Carver,
8. N. J. Warwick,
9. J. A. Pyle

, Reconciling the changes in atmospheric methane sources and sinks between the Last Glacial Maximum and the pre-industrial era. *Geophys. Res. Lett.* **38**, (2011). doi:10.1029/2011GL049545

ACCESSible BY



[UC-eLinks](#)[CrossRef](#)[Google Scholar](#)

50.

1. I. K. Seierstad,
2. P. M. Abbott,
3. M. Bigler,
4. T. Blunier,
5. A. J. Bourne,
6. E. Brook,
7. S. L. Buchardt,
8. C. Buizert,
9. H. B. Clausen,
10. E. Cook,
11. D. Dahl-Jensen,
12. S. M. Davies,
13. M. Guillevic,
14. S. J. Johnsen,
15. D. S. Pedersen,
16. T. J. Popp,
17. S. O. Rasmussen,
18. J. P. Severinghaus,
19. A. Svensson,
20. B. M. Vinther

, Consistently dated records from the Greenland GRIP, GISP2 and NGRIP ice cores for the past 104 ka reveal regional millennial-scale $\delta^{18}\text{O}$ gradients with possible Heinrich event imprint. *Quat. Sci. Rev.* **106**, 29–46 (2014). doi:10.1016/j.quascirev.2014.10.032

ACCESSIBLE BY

 BERKELEY
UNIVERSITY OF CALIFORNIA

[UC-eLinks](#) [CrossRef](#) [Google Scholar](#)

51.

1. S. O. Rasmussen,
2. M. Bigler,
3. S. P. Blockley,
4. T. Blunier,
5. S. L. Buchardt,
6. H. B. Clausen,

7. I. Cvijanovic,
8. D. Dahl-Jensen,
9. S. J. Johnsen,
10. H. Fischer,
11. V. Gkinis,
12. M. Guillevic,
13. W. Z. Hoek,
14. J. J. Lowe,
15. J. B. Pedro,
16. T. Popp,
17. I. K. Seierstad,
18. J. P. Steffensen,
19. A. M. Svensson,
20. P. Vallelonga,
21. B. M. Vinther,
22. M. J. C. Walker,
23. J. J. Wheatley,
24. M. Winstrup

, A stratigraphic framework for abrupt climatic changes during the Last Glacial period based on three synchronized Greenland ice-core records: Refining and extending the INTIMATE event stratigraphy. *Quat. Sci. Rev.* **106**, 14–28 (2014). doi:10.1016/j.quascirev.2014.09.007

 UC-eLinks [CrossRef](#) [Google Scholar](#)

52.

1. J. Ahn,
2. E. J. Brook,
3. A. Schmittner,
4. K. Kreutz

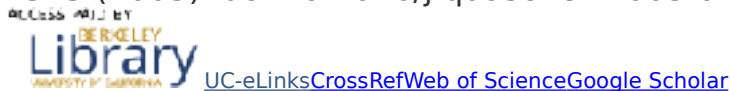
, Abrupt change in atmospheric CO₂ during the last ice age. *Geophys. Res. Lett.* **39**, (2012). doi:10.1029/2012GL053018

 UC-eLinks [CrossRef](#) [Google Scholar](#)

53. [↩](#)

1. E. J. Brook,
2. J. W. C. White,
3. A. S. M. Schilla,
4. M. L. Bender,
5. B. Barnett,
6. J. P. Severinghaus,
7. K. C. Taylor,
8. R. B. Alley,
9. E. J. Steig

, Timing of millennial-scale climate change at Siple Dome, West Antarctica, during the last glacial period. *Quat. Sci. Rev.* **24**, 1333-1343 (2005). doi:10.1016/j.quascirev.2005.02.002



54. **Acknowledgments:** This work was supported by NSF grants 1043518, 1142041, 0944552, 0839093, and 1142166. Data will be made available at <http://nsidc.org/data/> and <http://ncdc.noaa.gov/paleo/>. L. Layman, N. Chellman, D. Pasteris, M. Sigl, and C. Stowasser assisted with measurements. Thanks to J. Ahn for collated Siple Dome CH₄ data, J. Rosen for use of the Oregon State University firn air model, and T. Sowers for fruitful discussion. The authors appreciate the support of the WAIS Divide Science Coordination Office at the Desert Research Institute of Reno Nevada and the University of New Hampshire for the collection and distribution of the WAIS Divide ice core and related tasks (NSF grants 0230396, 0440817, 0944348, and 0944266). We are grateful to all participants in the field effort led by K. Taylor. The NSF Office of Polar Programs also funded the Ice Drilling Program Office and Ice Drilling Design and Operations group, the National Ice Core Laboratory, Raytheon Polar Services, and the 109th New York Air National Guard.

[View Abstract](#)